Biogeosciences Discuss., https://doi.org/10.5194/bg-2018-322
Manuscript under review for journal Biogeosciences
Discussion started: 8 August 2018

Biogeosciences Discussions Open Access EGU

Quantifying energy use efficiency via maximum entropy production: A case study from longleaf pine ecosystems

Susanne Wiesner[1], Christina L. Staudhammer[1], Paul C. Stoy[2], Lindsay R. Boring[3,4], Gregory Starr[1]
[1]Department of Biological Sciences, University of Alabama, Tuscaloosa, AL. 35487. USA.
[2]Department of Land Resources and Environmental Sciences, Montana State University, Bozeman, MT 59717, USA
[3]Jones Ecological Research Center, Newton, GA 39870, USA.
[4]Odum School of Ecology, University of Georgia, Athens, GA, 30602, USA

Correspondence to: Gregory Starr (gstarr@ua.edu)

Abstract. Global ecosystems vary in their function, and therefore resilience to disturbance, as a result of their location on Earth, structure, and anthropogenic legacy. Resilience can therefore be difficult to describe solely based on energy partitioning, as it fails to effectively describe how ecosystems use available resources, such as soil moisture. Maximum entropy production (MEP) has been shown to be a better metric to describe these differences as it relates energy use efficiencies of ecosystems to the availability of resources. We studied three sites in a longleaf pine ecosystem with varying levels of anthropogenic legacy and biodiversity, all of which were exposed to extreme drought. We quantified their resilience from radiative, metabolic and overall MEP ratios. Sites with anthropogenic legacy had ~10% lower overall and metabolic energy use efficiency compared to more biodiverse sites. This resulted in lower resilience and a delay in recovery from drought by ~1 year. Additionally, a set of entropy ratios to determine metabolic and overall energy use efficiency explained more clearly site-specific ecosystem function, whereas the radiative entropy budget gave more insights about structural complexities at the sites. Our study provides foundational evidence of how MEP can be used to determine resiliency across ecosystems globally.

1 Introduction

Energy use efficiency in ecosystems comprises the efficient utilization and conversion of resources, such as solar radiation, nutrients and water (Amthor, 2010; Beer et al., 2009; Finzi et al., 2007; Thomas et al., 2016). Understanding the elements affecting energy use efficiencies is crucial, as anthropogenic and climate induced changes around the globe threaten to alter resources and the ability of ecosystems to utilize them (Haddeland et al., 2014; Porter et al., 2012; Reinmann and Hutyra, 2016; Thom et al., 2017).

Ecosystem energy use efficiency is often described based on the ability of the system to partition energy into sensible and latent heat fluxes (Huryna and Pokorny, 2016; Ripl, 1995; Wilson, 2002). However, energy fluxes differ substantially within and among ecosystems, due to differences in structure and function (Kang et al., 2015), which regulate their base rate of energy use (Brunsell et al., 2011). For example, ecosystems exhibit small-scale changes in environmental variables based on their structural properties (Perry, 2002). This spatial heterogeneity can drive differences in microclimate which lead to

Biogeosciences Discuss., https://doi.org/10.5194/bg-2018-322
Manuscript under review for journal Biogeosciences
Discussion started: 8 August 2018

changes in the turbulent exchange between the land and atmosphere (Perry, 2002). Additionally, differences in initial conditions during the development of ecosystems can have large impacts on their trajectory (e.g. "butterfly-effect;"; Dantas-Torres, 2015; Hastings, 1993). The combination of these factors leads to different baselines of energy use efficiency and may even cause instabilities in ecosystems as they further develop (Mori, 2011). Complicating our understanding of ecosystem energy dynamics is the fact that more frequent fluctuations in environmental variables are expected as a result of global climate change, including extreme events like droughts, which will alter the resource efficiency of ecosystems across the globe and with it their resilience (Franklin et al., 2016; Woodward et al., 2010). This has the potential to further intensify instabilities, which may shift or disrupt the dynamic equilibriums of ecosystems (Mori, 2011; Siteur et al., 2016).

The use of maximum entropy production (MEP) has been proposed as a metric to address ecosystem energy use efficiency (Kleidon et al., 2010; Stoy et al., 2014; Swenson, 1989) based on the notion that the second law of thermodynamics can be applied to whole ecosystems to describe their strategy for resource utilization (e.g. carbon and water fluxes; Dewar, 2005; Whitfield, 2005; 2007). It is hypothesized that ecosystems aim to optimize their energy use and thus maximize their entropy production to avoid thermodynamic equilibrium. MEP is therefore thought to be the most probable outcome of the different ways elements in non-equilibrium can reorganize themselves (Jaynes, 1957b; 1957a), corresponding to a dynamic stable state of an ecosystem with its surroundings (Dyke and Kleidon, 2010; Schneider and Kay, 1994; Svirezhev, 2000). Hence, the principle of MEP allows us to make the least unlikely projection of a system responding to any kind of change (Endres, 2017; England, 2015).

The magnitude of entropy production depends on the thermodynamic gradients (i.e., thermal, chemical, etc.) between organisms and their surroundings (Kleidon, 2010). Ecosystems invest energy to build more complex structures (i.e., self-sustainability; Müller and Kroll, 2011; Virgo and Harvey, 2007), which enhances their entropy efficiency (Odum, 1988; Schneider and Kay, 1994). For example, more vertically structured stands were found to be more efficient in harvesting available light, which consequently increased their productivity (Bohn and Huth, 2017; Hardiman et al., 2011). Yet, anthropogenic modifications threaten to change the structural integrity of ecosystems and therefore their ability to build thermodynamic gradients. For example, agricultural systems were shown to exceed MEP, due to the application of fertilizer and periodic irrigation schedules (i.e., artificial energy; Patzek, 2008; Steinborn and Svirezhev, 2000). This excessive entropy production is unsustainable and decreases the ability of ecosystems to adapt to perturbations (Cochran et al., 2016). This is because agricultural practices compensate for natural fluctuations in resource availability, which would normally encourage higher resilience (Brookes et al., 2005), through the application of artificial energy (Patzek, 2008).

Here, we evaluate how efficiently ecosystems use incoming energy by assessing individual components of an ecosystem's entropy production in comparison to the empirical MEP of the system (Stoy et al., 2014). We do so by measuring the structural complexity of an ecosystem, via the enhanced vegetation index (EVI) and variations in understory structure, in relation to the entropy partitioning of incoming energy from solar radiation. For example, sites with greater leaf area, and therefore higher EVI, can maintain higher latent energy (LE) fluxes, which increase entropy production (Meysman and Bruers, 2010), as LE couples both mass and energy cycles (Brunsell et al., 2011). In addition, high entropy production from

LE results in greater photosynthetic capacity, which enables maintenance of structural components (Marín et al., 2014). On the contrary, ecosystems that dissipate entropy more through sensible heat fluxes (H) can rapidly deplete the temperature gradient between the surface and canopy, which would eventually lead to lower entropy production (LeMone et al., 2007).

Here we build upon the techniques proposed by Stoy et al. (2014), Holdeway et al. (2010) and Brunsell et al. (2011) by calculating entropy ratios to compare and contrast three sites (mesic, intermediate and xeric) within a longleaf pine (*Pinus palustris* Mill.) ecosystem. The three longleaf pine sites differed in ecosystem structure (i.e., basal area, EVI, etc.; Table 1) and biodiversity based on differences in soil water holding capacity, as well as different levels of anthropogenic legacy. The sites were exposed to a severe drought in the beginning of this study, which we used to quantify ecosystem resilience through the calculation of entropy efficiency ratios. We focused on entropy production from the absorption of radiation (eff_{rad}) and metabolic activity (eff_M), as well as overall ecosystem function (i.e., entropy production from LE, H, metabolism and radiation; eff_s).

We hypothesize that (1) the xeric site will have a higher entropy flux from sensible heat (J_H) due to its lower vegetation coverage and lower basal area, and therefore higher partitioning into H rather than LE, which will lower its overall entropy efficiency compared to the mesic site, (2) the mesic site will be able to maintain higher entropy efficiencies (eff_{rad}, eff_M and eff_s) due to its structural complexity (i.e., species diversity and basal area), and (3) the intermediate site will have lower eff_{rad}, eff_s and eff_M compared to the mesic and xeric sites, as a result of its lower biodiversity and structural complexity, a consequence of its anthropogenic legacy.

We show that a combination of different entropy efficiency ratios revealed how structural and functional characteristics in this ecosystem contribute to energy use efficiencies at the three sites. Our results demonstrate that resilience to disturbance is a function of entropy efficiency, as low efficiencies at anthropogenically altered sites prolonged the recovery from drought by approximately a year. In contrast, more biodiverse stands (in overstory and understory) were able to maintain high entropy/energy use efficiencies, which increased their resilience to and recovery from drought.

2 Materials and Methods

2.1 Site description

This study was conducted at the Joseph W. Jones Ecological Research Center in southwestern Georgia, USA (31.2201° N, 84.4792° W) from January 2009 to December 2016. The three sites are maintained by frequent low intensity fire on a two-year return interval and were last burned in 2015 (Starr et al., 2016). The climate is humid subtropical with a mean annual precipitation of 1310 mm (Kirkman et al., 2001). Mean temperature extremes range from 3 °C to 16 °C in winter and 22 °C to 33 °C in summer (NCDC, 2011).

The three sites differ based on soil moisture availability, as a result of differences in soil drainage. The mesic site lies on somewhat poorly drained sandy loam over sandy clay loam and clay textured soils (Goebel et al., 1997; 2001). Soils at the intermediate site are well drained and have a depth to the argillic horizon of ~165 cm (Goebel et al., 1997). The xeric site lies

on well-drained deep sandy soils with no argillic horizon (Goebel et al., 1997). All sites are situated within 10 km of each other with average elevations of 165, 155, and 160 m for the mesic, intermediate, and xeric sites, respectively.

95-year-old longleaf pine trees (*Pinus palustris* Mill.) dominate the overstory of all sites, and overall basal area (B_A) and diameter at breast height (DBH) varied by site (Table 1). The xeric site has the highest proportion of oak trees in the overstory with 22 %, versus 8 % and 7.7 % at the mesic and intermediate sites, respectively. The understory at the mesic and xeric sites is largely covered with perennial C_4 grass species, such as wiregrass (*Aristida beyrichiana* [Trin.]), whereas woody species dominate at the intermediate site. The composition and abundance of other overstory and understory species varies by site (Kirkman et al., 2001; 2016). Soil perturbation at the intermediate site affected species richness, so that wiregrass is almost absent, resulting in an understory dominated by woody species.

We acquired monthly EVI for 2009 through 2016 for all three sites from the online data pool at lpdaac.usgs.gov via the NASA Land Processes Distributed Active Archive Center (LP DAAC) and the USGS Earth Resources Observation and Science Center (EROS), using MODIS Aqua and Terra data products (MYD13Q1 and MOD13Q1; DAAC, 2008) to quantify changes in ecosystem structure from disturbance. We also acquired Palmer Drought Severity Indices (PDSI) for Southwest Georgia from the National Oceanic and Atmospheric Administration data archive for 2009 to 2016 to identify the months of drought disturbance (Dai et al., 2004).

Net ecosystem exchange of CO_2 measurements. Net ecosystem exchange (NEE) was measured continuously at 10 Hz at all three sites from January 2009 to December 2016 using open-path eddy covariance (EC) techniques (Whelan et al., 2013). The data was stored on CR-5000 dataloggers (Campbell Scientific, Logan, UT). CO_2 and water vapor concentration were measured with an open path infrared gas analyzer (IRGA, LI-7500, LI-COR Inc., Lincoln, NE) and wind velocity and sonic temperature were measured with a three-dimensional sonic anemometer (CSAT3, Campbell Scientific, Logan, UT). These sensors were installed ~4 m above mean canopy height at each site (34.5, 37.5, and 34.9 m for the mesic, intermediate and xeric sites, respectively), ~0.2 m apart to minimize flow distortion between the two instruments and vertically aligned to match the sampling volume of both instruments.

2.2 Sensible and latent heat flux measurements

Net energy fluxes of LE and H were estimated in W m^{-2} using temperature and wind velocity measurements from the sonic anemometer, as well as water vapor density measurements from the IRGA:

$$\mathrm{LE} = \lambda \rho_a \overline{w'q'} \quad (1.1)$$

$$\mathrm{H} = \rho_a c_p \left(\overline{w'T_s'} - 0.000321 T_s \overline{w'q'}\right) \quad (1.2)$$

where λ is the latent heat of vaporization (J kg^{-1}), ρ_a is the density of air (kg m^{-3}), c_p is the specific heat of air (kJ kg_{-1} K^{-1}), w' is the instantaneous deviation of vertical wind speed (w, m s^{-1}) from the mean, and q' and T_s' are the instantaneous deviations of water vapor concentration (kg kg^{-1}) and sonic temperature (Kaimal and Gaynor, 1991) from their respective

means. The overbars in Eqs. 1.1 and 1.2 signify the time-averaged covariance. Missing H and LE were gap-filled using simple linear models on a monthly basis regressed with net radiation.

For entropy calculations, H and LE were corrected using the Bowen method following Twine *et al*. (2000), where the fluxes were adjusted using residual energy of net radiation (R_n) when subtracting ground heat flux (G), and the estimated Bowen ratio from H and LE ($\beta = H/LE$), under the assumption that β was correctly measured by the EC system. The corrected values of LE and H were then:

$$LE = \frac{1}{1+\beta}(R_n - G) \quad (1.3)$$

$$H = \beta \times LE \quad (1.4)$$

2.3 Meteorological instrumentation

Meteorological data were collected and stored on CR-5000 dataloggers (Campbell Scientific, Logan, UT). Meteorological data measured on the towers included: photosynthetically active radiation (PAR; LI-190, LI-COR Inc., Lincoln, NE), global radiation (LI-200SZ, LI-COR Inc., Lincoln, NE), incident and outgoing shortwave and longwave radiation to calculate R_n (NR01, Hukseflux, thermal sensors, Delft, The Netherlands), precipitation (TE525 Tipping Bucket Rain Gauge, Texas Electronics, Dallas, TX), wind direction and velocity (Model 05103-5, R.M. Young, Traverse City, MI), air temperature (T_{air}) and relative humidity (RH; HMP45C, Campbell Scientific, Logan, UT), and barometric pressure (PTB110, Vaisala, Helsinki, Finland).

Soil temperature (T_{soil}), volumetric water content of the soil (SWC) and G were measured in one location near the base of each tower at each site every 15 seconds and averaged every 30 minutes on an independently powered CR10X datalogger. T_{soil} was measured at depths of 4 and 8 cm with insulated thermocouples (Type-T, Omega Engineering, INC., Stamford, CT), and G was measured at a depth of 10 cm with soil heat flux plates (HFP01, Hukesflux, Delft, The Netherlands). SWC was measured within the top 20 cm of the soil surface using a water content reflectrometer probe (CS616, Campbell Scientific, Logan, UT).

2.4 Data processing

Raw EC data were processed using EdiRe (v.1.4.3.1184; Clement, 1999), which carried out a 2-d coordinate rotation of the horizontal wind velocities to obtain turbulence statistics perpendicular to the local streamline. Fluxes were calculated for half-hour intervals and then corrected for mass transfer resulting from changes in density not accounted for by the IRGA. Barometric pressure data were used to correct fluxes to standard atmospheric pressure. Flux data screening was applied to eliminate 30-min fluxes of NEE, H and LE, resulting from systematic errors as described in Whelan et al. (2013) and Starr et al. (2016). Such errors encompassed (amongst other things): rain, poor coupling of the canopy and the atmosphere (defined by the friction velocity, ustar), and excessive variation from half-hourly means.

Biogeosciences Discuss., https://doi.org/10.5194/bg-2018-322
Manuscript under review for journal Biogeosciences
Discussion started: 8 August 2018

Gross ecosystem exchange (GEE) and ecosystem respiration (R_{eco}) were estimated from eddy covariance measurements of net ecosystem exchange of CO_2 (NEE; μmol m^{-2} s^{-1}) at a time resolution of half an hour, from which GEE and R_{eco} can be estimated as follows:

$$GEE = -NEE + R_{eco} \quad (2)$$

Missing half hourly data were gap-filled using separate functions for day and night as described in Whelan *et al.* (2013) and Starr *et al.* (2016).

2.5 Entropy production calculations

LE, H, and G fluxes were converted from W m^{-2} to kJ m^{-2} and summed to monthly estimates. Net ecosystem exchange of CO_2 was converted to kJ m^{-2}, using the assumption that one micromole of CO_2 stores approximately 0.506 J (Nikolov et al., 1995), and then summed to monthly metabolic energy values.

For entropy production and fluxes of shortwave (R_s) and longwave radiation (R_l) we followed established approaches of Brunsell *et al.* (2011), Holdaway *et al.* (2010), and Stoy *et al.* (2014). The entropy flux produced through emission of R_s at the surface of the sun (J_{Rs}, kJ m^{-2} K^{-1}) was calculated as:

$$J_{Rs} = \frac{R_{s,in}}{T_{sun}} \quad (3.1)$$

where sun surface temperature (T_{sun}) was assumed to be ~5780 K, with $R_{s,in}$ defined as incident R_s. For entropy flux of R_l (J_{Rl}, kJ m^{-2} K^{-1}), we calculated:

$$J_{Rl} = \left(\frac{R_{l,in}}{T_{sky}} - \frac{R_{l,out}}{T_{srf}}\right) \quad (3.2)$$

where $R_{l,in}$ is incoming R_l, $R_{l,out}$ is outgoing R_l, and surface temperature (T_{srf}; K) was calculated from upwelling R_l:

$$T_{srf} = {R_{l,out}}\Big/{(A \times e_{srf} \times k_B)^{\frac{1}{4}}} \quad (3.2.1)$$

with emissivity of the surface calculated as e_{srf} = 0.99-0.16α (Juang et al., 2007), the surface area A was 1 m^2, and the Stefan-Boltzmann constant k_B = 5.67 × 10^{-8} W m^{-2} K^{-4}. The shortwave albedo (α) was calculated as the monthly average of noontime $R_{s,out}$, defined as outgoing R_s, divided by $R_{s,in}$. The sky temperature, T_{sky} (K), was calculated from $R_{L,in}$ using the Stefan-Boltzmann equation:

$$T_{sky} = {R_{l,in}}\Big/{(A \times e_{atm} \times k_B)^{\frac{1}{4}}} \quad (3.2.2)$$

where the emissivity of the atmosphere (e_{atm}) was assumed to be 0.85 for R_l, following Campbell and Norman (1998).

All other ecosystem entropy fluxes J_{LE}, J_H, J_G, and J_{NEE} (kJ m^{-2} K^{-1}) were calculated by dividing the energy fluxes by temperature as:

$$J_x = \frac{x}{T_y} \quad (3.3)$$

Biogeosciences Discuss., https://doi.org/10.5194/bg-2018-322
Manuscript under review for journal Biogeosciences
Discussion started: 8 August 2018

where x = LE, H, G and NEE_e, and y = T_{air} (for J_{LE}, J_H and J_{NEE}; K) or T_{soil} (for J_G). We used the energy of NEE (NEE_e) directly measured with the EC towers, to calculate change in entropy of the metabolic system.

We also calculated entropy produced from evaporation associated with mixing of saturated air from the canopy with the fraction of air in the atmosphere that has RH below 100 % (JLE_{mix}), following Holdaway *et al*. (2010):

$$JLE_{mix} = ET \times R_v \times ln(RH) \quad (3.4)$$

where the evapotranspiration rate, ET = LE/λ, λ is the latent heat of vaporization of water, and R_v is the gas constant of water vapor (0.461 kJ kg^{-1} K^{-1} for moist air).

The sum of entropy of ecosystem fluxes (J, kJ m^{-2} K^{-1}) was then calculated by adding all entropy fluxes between the surface and atmosphere:

$$J = J_{Rl} + J_{Rs} + J_{LE} + J_H + J_G + J_{NEE} + JLE_{mix} \quad (3.5)$$

The conversion of low entropy R_s and R_l to high entropy heat at the surface through absorption of R_s and R_l, respectively, was calculated as:

$$\sigma_{Rs} = R_{s,net}\left(\frac{1}{T_{srf}} - \frac{1}{T_{sun}}\right) \quad (3.6)$$

$$\sigma_{Rl} = R_{l,net}\left(\frac{1}{T_{srf}} - \frac{1}{T_{sky}}\right) \quad (3.7)$$

where T_{srf} is the radiometric surface temperature (Eq. 3.2.1) and σ_{RS} and σ_{Rl} are in kJ m^{-2} K^{-1}.

The overall entropy production (σ, kJ m^{-2} K^{-1}) was then calculated as the sum of the entropy productions of R_s and R_l:

$$\sigma = \sigma_{Rl} + \sigma_{Rs} \quad (3.8)$$

Finally, we estimated overall change in entropy production (S) over time (t) in kJ m^{-2} K^{-1} of the ecosystem by adding entropy flux and entropy production:

$$dS/dt = J + \sigma \quad (3.9)$$

Note that this approach does not account for entropy production due to frictional dissipation of entropy from rainfall or subsurface water flow, as these would be of even smaller magnitude than entropy production from metabolic activity of the ecosystem (Brunsell et al., 2011).

2.6 MEP calculations

We estimated MEP of the radiation budget (MEP_{rad}), metabolic entropy budget (MEP_M), and overall entropy (MEP_s) in kJ m^{-2} K^{-1}, to compare their effectiveness in quantifying ecosystem function.

MEP of the radiation budget (MEP_{rad}) was determined following Stoy *et al*. (2014), by estimating the MEP of R_s (MEP_{Rs}) and R_l (MEP_{Rl}):

$$MEP_{Rs} = R_{s,in}\left(\frac{1}{T_{air}} - \frac{1}{T_{sun}}\right) \quad (4.1)$$

$$MEP_{Rl} = R_{l,net}\left(\frac{1}{T_{srf}} - \frac{1}{T_{air}}\right) \quad (4.2)$$

Biogeosciences Discuss., https://doi.org/10.5194/bg-2018-322
Manuscript under review for journal Biogeosciences
Discussion started: 8 August 2018

$$MEP_{rad} = MEP_{Rs} + MEP_{Rl} \quad (4.3)$$

We assume that under ideal conditions, an ecosystem maximizes its entropy production when it converts all incoming R_s and R_l into work (Stoy et al., 2014). Note that MEP_{Rl} is often negative or 0 because an efficient ecosystem would convert less energy into sensible heat, such that T_{srf} would approach T_{air}.

The entropy efficiency ratio of radiation is then calculated using σ of the radiation from Eq. 3.8 as follows:

$$eff_{rad} = \frac{\sigma}{MEP_{rad}} \quad (4.4)$$

Maximum entropy of metabolism, as the metabolic energy use efficiency, was calculated by estimating maximum possible entropy production assuming that the ecosystem would be able to use all incoming energy from GEE (E_{in}) as a function of T_{air} (K) and therefore maximize its entropy dissipation:

$$MEP_M = \frac{E_{in}}{T_{air}} \quad (4.5)$$

The entropy efficiency ratio of metabolism was then calculated from metabolic entropy flux of actual available energy J_{NEE}, estimated as NEE_e/T_{air} (in K), divided by MEP_M:

$$eff_M = \frac{J_{NEE}}{MEP_M} \quad (4.6)$$

Maximum entropy of all energy fluxes (MEP_s) was assumed as the maximum efficiency of an ecosystem, if all incoming energy from R_s and R_l was converted to work, which would only depend on T_{srf}:

$$MEP_s = \frac{R_{s,in}}{T_{srf}} + \frac{R_{l,in}}{T_{srf}} \quad (4.7)$$

We then estimated overall site entropy efficiency as:

$$eff_s = \frac{dS/dt}{MEP_s} \quad (4.8)$$

2.7 Statistical analyses

We tested for significant differences in environmental and structural variables among the three sites prior to the entropy analysis. We estimated simple general linear mixed models (GLMM) to look at differences among sites and of SWC, vapor pressure deficit (VPD), EVI, albedo, T_{srf}, T_{air} and T_{sky}, as well as $R_{s,in}$, $R_{s,out}$, $R_{l,in}$ and $R_{l,out}$ via the R function *nmle*. All response variables were monthly means except for rainfall and the radiation components, which were monthly sums. We used a generalized linear model to analyze rainfall sums, utilizing a quasi-Poisson distribution with a log function to link linear predictors to the mean of the response variable via the function *glm* in R. We included a random effect for year and month, to account for repeated measurements, as well as an AR(1) structure to account for possible temporal autocorrelation among measurements. Independent variables were month, year and site, as well as their interactions.

Subsequently, we estimated GLMMs of monthly entropy fluxes (J_{LE}, J_H, J_G, and J_{NEE}), entropy production (σ), and entropy efficiency ratios (eff_{rad}, eff_s, and eff_M) to quantify differences by environmental and structural variables and by site. As in the models of environmental variables, we included random effects and an AR(1) autoregressive correlation structure to account

for repeated monthly measurements. All models initially included independent variables for site, year and month, mean monthly T_{air} (except for J_G, which included T_{soil}), SWC, rainfall, VPD and EVI, as well as their interactions with site. We also included the interactions of site with year, to determine changes in the energy efficiency pre, during and post drought at the three sites. Independent variables and their interactions were deemed significant when $p<0.05$. We used a Tukey adjustment to test for significant differences among sites. We also calculated cumulative sums of the entropy efficiency ratios (i.e., eff_{rad}, eff_M, eff_s) to quantify the total difference among the sites over the course of this study. Analyses were performed via the R packages *nlme*, *lsmeans*, and *car* (Fox and Weisberg, 2011; Lenth, 2016; Pinheiro et al., 2014).

3 Results

3.1 Differences in environmental, radiative and temperature variables among sites

All three sites experienced a severe drought from mid-2010 through mid-2012 (Fig. 1). Rainfall decreased (by ~50 mm per month) and VPD increased during the drought on average by ~ 0.4. SWC was significantly lower at the xeric (<20 %) compared to mesic and intermediate sites (~20 %) for all years of this study, but decreased more at the mesic and intermediate site during the drought. EVI was on average 0.02 lower at the xeric site compared to the other two sites, which was significant for all years compared to the mesic, except for 2011, 2013 and 2016; and compared to the intermediate site except for 2013. During the drought EVI decreased at all sites, which was only significant at the mesic site (Fig. 1).

The albedo was significantly lower at the xeric site (~0.125), but did not differ between the mesic and intermediate sites (~0.108) for 2009 and 2010. The albedo increased at the mesic and intermediate sites, but decreased at the xeric site during the beginning of the drought to 0.115 and 0.125, respectively (Fig. 1). Values for albedo were not significantly different between the intermediate and xeric sites following 2010, but the albedo at the mesic site was significantly lower compared to the other sites following 2011 (Fig. 1).

T_{srf} at the xeric increased above that of the mesic site in 2009 and 2015. In 2016 the intermediate site had significantly higher T_{srf} compared to the mesic site. T_{air} was significantly lower at the mesic compared to the intermediate site for the years 2009, and 2014 - 2016. In addition, the xeric had higher T_{air} compared to the mesic site in 2012, 2013 and 2015. T_{air} at the xeric site decreased below that of the intermediate during 2014 and 2015. For the years 2012, 2013, and 2015 the mesic site had significantly lower T_{air} compared to the xeric (Fig. 1). T_{sky} at the intermediate site was significantly lower compared to the mesic in 2009 through 2014. The xeric site had significantly higher T_{sky} compared to the mesic during 2012 - 2016 and compared to the intermediate site for all years of this study (Fig. 1).

We did not find any significant differences in $R_{s,in}$ by site. However, we did see significant differences in $R_{s,out}$, $R_{l,in}$ and $R_{l,out}$, with less $R_{l,out}$ at the mesic site compared to the intermediate site, and significantly more $R_{l,in}$ at the xeric site, compared to the mesic site (Fig. 2). Monthly $R_{s,out}$ was higher at the xeric site from 2009 through 2011, compared to the other two sites (Fig. 2). From 2012 on, the mesic site had significantly lower $R_{s,out}$ compared to the other two sites.

Biogeosciences Discuss., https://doi.org/10.5194/bg-2018-322
Manuscript under review for journal Biogeosciences
Discussion started: 8 August 2018

3.2 Understory wiregrass and woody abundance at the sites

Wiregrass was virtually absent at the intermediate site for all years of this study (Fig. 3), whereas woody species were significantly more abundant at that site compared to the mesic and xeric sites. The mesic and xeric sites both had significantly higher proportions of wiregrass in the understory (~25 % versus 5 % at the intermediate site), which slightly decreased during 2011 (Fig. 3). During 2011, woody biomass increased to ~75 g m^{-2} at the xeric site, but not at the mesic site. In 2012, woody biomass decreased to ~40 g m^{-2} at the xeric and intermediate sites and remained low during the following years at the xeric site, but increased at the intermediate site (>100 g m^{-2}).

3.3 Changes in the entropy fluxes of J_H, J_{LE}, and J_{NEE} and J_G and entropy production

The xeric site had significantly higher monthly J_{LE}, ranging from ~650 to 750 kJ m^{-2} K^{-1}, versus the intermediate site with ~480-600 kJ m^{-2} K^{-1} (Fig. 4) for all years except 2014. J_{LE} at the xeric site was also higher than the mesic site in 2011-2013 and 2015, ranging from 550 to 650 kJ m^{-2} K^{-1} per month. The mesic site had ~100-150 kJ m^{-2} K^{-1} higher J_{LE} compared to the intermediate in 2010, 2012 and 2016. J_{LE} significantly increased with greater T_{air}, SWC (data not shown) and EVI (Fig. 4), independent of site. J_{LE} was significantly higher at the mesic site, compared to the intermediate site when VPD was above 0.4 (Fig. 4). The xeric site had significantly greater J_{LE} compared to the mesic site when VPD was below 1 kPa, and significantly greater J_{LE} compared to the intermediate site when VPD was below 1.5 kPa.

J_H was significantly higher at the mesic site in 2011 and 2015 (~400-500 kJ m^{-2} K^{-1}) compared to the intermediate (~ 500-600 kJ m^{-2} K^{-1}; Fig. 4) and xeric sites (~550-700 kJ m^{-2} K^{-1}). In 2012 the xeric site had significantly lower J_H compared to the other sites (by ~ 100 kJ m^{-2} K^{-1}) and in 2016 the mesic site had significantly lower J_H compared the intermediate site (by ~100 kJ m^{-2} K^{-1}). J_H decreased with increasing SWC (data not shown) and EVI (Fig. 4) and was significantly higher with increasing T_{air}, independent of site. VPD significantly increased J_H at all three sites. J_H was significantly lower at that xeric site compared to the mesic and intermediate sites when VPD was below 0.4 kPa (Fig. 4).

J_{NEE} was always negative at the mesic site throughout this study, indicating more energy storage which decreased entropy production locally (Fig. 4). The mesic site had significantly lower J_{NEE} compared to the intermediate site for all years, except 2011, and 2015. The mesic site had significantly more negative J_{NEE} compared to the xeric site in 2009 and 2012, whereas the xeric site had significantly more negative J_{NEE} compared to the intermediate site for the years 2010, and 2012-2014. The mesic site had significantly more negative J_{NEE} compared to the other two sites when EVI was below 0.35 (Fig. 4). In addition, the xeric site had less positive J_{NEE} (by ~ 1 kJ m^{-2} K^{-1}) compared to the intermediate site when EVI was <0.44. For T_{air} between 17-23 °C, the mesic site had significantly more negative J_{NEE} compared to the xeric site. When T_{air} was above 17 °C, J_{NEE} at the intermediate site was significantly more positive compared to the other sites (by > 2 kJ m^{-2} K^{-1}; Fig. 4). J_{NEE} became more negative (from -1 to -4 kJ m^{-2} K^{-1}) with increasing VPD, independent of site, and was not affected by SWC or rainfall (data not shown).

J_G was significantly higher at the xeric site, compared to the intermediate site in 2012. In 2016, J_G at the intermediate site (-35 kJ m^{-2} K^{-1}) was significantly more negative compared to the mesic and xeric sites (0-10 kJ m^{-2} K^{-1}; Fig. 5). In contrast, J_G was significantly more positive at the xeric site, compared to other sites when SWC was >22 %. J_G increased from negative to positive with an increase in T_{soil}, which was not significantly different by site (Fig. 5). J_G was not affected by VPD, rainfall or EVI.

In 2010, 2012 and 2013, σ was significantly higher at the mesic site compared to the xeric site (by > 50 kJ m^{-2} K-1; Fig. 5). In 2009, 2011 and 2012 σ was significantly higher at the intermediate site (by > 50 kJ m^{-2} K^{-1}) compared to the xeric, but not the mesic site (Fig 5). Entropy production was unaffected by SWC, T_{air}, and EVI, but significantly increased with higher VPD (from <1400 to 1800 kJ m^{-2} K^{-1}; Fig. 5).

3.4 Entropy efficiency ratio models

Values of eff_{rad} were significantly higher at the intermediate site, compared to the mesic and xeric sites in 2009, followed by no significant difference between the mesic and intermediate sites in 2010 and 2011 (Fig. 6). eff_{rad} was significantly higher at the mesic site (~0.9), compared to the intermediate (~0.89) site from 2012 through 2016, whereas eff_{rad} at the xeric site was significantly lower compared to the mesic and immediate sites throughout this study. There was no significant change in eff_{rad} at the mesic and intermediate sites in from 2009 through 2011, but eff_{rad} at the xeric site significantly increased starting 2010 throughout the remainder of this study. eff_{rad} at the mesic site significantly increased in 2012 and remained high (>0.9) for the remainder of this study. There was no significant change in eff_{rad} at the intermediate site in this study, with the exception of 2012, which was significantly lower compared to 2009 and 2015. Values of eff_{rad} were significantly greater when EVI increased, independent of site (Fig. 6). Values of eff_{rad} only significantly increased with increasing SWC at the mesic site and exhibited no significant change at the other two sites (Fig. 6). The mesic site had significantly higher, whereas the xeric site had significantly lower values of eff_{rad} compared to the other two sites for all levels of SWC and VPD. Higher VPD significantly decreased values of eff_{rad} only at the xeric site (Fig. 7). Values of eff_{rad} significantly increased with higher T_{air} only at the mesic and xeric sites (Fig. 7). The mesic site had higher values of eff_{rad} compared to the intermediate site when T_{air} was above 10 °C. The xeric site had significantly lower values of eff_{rad} compared to the other two sites for all levels of T_{air} (Fig. 7). Rainfall significantly decreased values of eff_{rad} by > 0.005 regardless of site (data not shown). The cumulative sum of eff_{rad} at the intermediate site exceeded 100 % of that at the mesic site up until the beginning of 2012 followed by consistent decreases below 99 % of eff_{rad} at the mesic site. During the drought the xeric site experienced a steep increase in eff_{rad} relative to the mesic site, ranging from 96.5-98 %, which remained at 98 % for the remainder of the study.

Values of eff_M were significantly higher at the mesic site compared to the intermediate for all years in this study except for 2015, and compared to the xeric for all years except for 2014 (Fig. 6). Values of eff_M were not significantly different between the intermediate and xeric sites. Values of eff_M did not significantly change throughout this study at the mesic and intermediate sites. At the xeric site eff_M was significantly higher in 2013, 2014 and 2016, compared to 2009. Values of eff_M significantly increased with increasing EVI at the intermediate and xeric sites, but not the mesic site (Fig. 6). The mesic site

had significantly higher eff_M compared to the other sites when EVI was below 0.4 (Fig. 6). The xeric site had significantly higher values of eff_M compared to the mesic site when EVI increased above 0.5. Values of eff_M were significantly higher at the mesic site compared to the other sites, when SWC was between 19 and 23 % (Fig. 7). When SWC was above 23 %, eff_M at the xeric site was significantly lower compared to the other sites (Fig. 7). Greater VPD significantly increased eff_M by ~0.1, whereas T_{air} significantly decreased eff_M by more than 0.1 independent of site (data not shown). Rainfall had no effect on E_M. The cumulative sum of eff_M at the intermediate and xeric sites ranged between 90-95 % and 71-94 % of eff_M at the mesic site, respectively. During the drought the intermediate site experienced a decrease in eff_M, whereas the xeric site experienced a constant increase in eff_M relative to the mesic site.

Values of eff_s were significantly higher at the mesic site, compared to the intermediate site for all years except 2013 and 2014 (by 0.02-0.04; Fig. 6). eff_s was significantly higher at the xeric site (by ~0.02) compared to the intermediate site for all years, except 2009, 2010 and 2014 (Fig. 6). While the mesic site had significantly higher eff_s compared to the intermediate for all levels of EVI (by ~ 0.02-0.025), the xeric was significantly higher (~0.45) than the intermediate site (~0.425) when EVI was above 0.22, and significantly lower than the mesic when EVI was below 0.25 (Fig. 6). eff_s significantly increased with higher SWC, VPD and T_{air} (by ~0.05-0.1), independent of site (data not shown). Rain had no effect on eff_s. The cumulative sum of eff_s at the intermediate site was ~97 % of that at the mesic site during the drought, which then decreased to 96 % for the remainder of this study. Similar to the relative cumulative sum of eff_{rad} and eff_M, the xeric site experienced an increase in the cumulative sum of eff_s relative to the mesic site, ranging from 90 to 97 %.

4 Discussion

Here we describe differences in energy use efficiencies of sites with varying structural complexities (i.e., understory composition, basal area, DBH) using entropy fluxes and production and entropy efficiency ratios. We show that more structurally complex sites – namely the xeric and mesic sites – have higher metabolic and overall energy use efficiencies compared to a site with anthropogenic modifications (i.e., intermediate site). Although the radiation entropy efficiency (eff_{rad}) indicated that both the mesic and intermediate sites were equally energy efficient, eff_s and eff_M revealed lower ecological function at the intermediate site. From these results we conclude that a combination of entropy efficiency ratios can give more valuable insights about the energy use efficiency and resiliency of ecosystems, as opposed to focusing only on individual parts of the entropy budget.

We hypothesized that the xeric site would have higher J_H, due to its sparser canopy and sandy soils and therefore lower volumetric heat capacity, in addition to the effect of lower soil water availability. However, in contrast to our first hypothesis, the mesic and intermediate sites and not the xeric site experienced a more severe increase in J_H when EVI decreased during the disturbance of drought (Fig. 1). Furthermore, the effect of SWC and rainfall on J_H was not significantly different by site, suggesting that plant transpiration, and thus the cooling of leaf surfaces, was the driving force for changes in J_H and not differences in water availability. Furthermore, even though plant abundance was lower at the xeric site, its

species composition was better adapted to drought conditions, which allowed for the preservation of J_{LE}. In contrast, the mesic site was affected by the interaction of physical (i.e., albedo; Fig. 1) and biological forces, as albedo increased with decreasing plant biomass (lower EVI), which was not observed at the xeric site (Fig. 1). As a consequence, J_{LE} decreased during the drought, which resulted in lower overall entropy efficiency (Fig. 6). eff_s decreased due to lower leaf area at the mesic site, which resulted in more radiation reaching the ground, thereby increasing T_{srf} (Figs. 1 and 2) and evaporation of water from the soil. This depleted soil moisture storage (Fig. 1) and therefore decreased plant hydraulics and with it J_{LE} (Kim and Wang, 2012; Lauri et al., 2014), which caused a shift in the energy balance to higher rates of J_H. Additionally, the xeric site experienced more J_{LE} compared to the intermediate site, even though its basal area was almost half that of the intermediate (Table 1). This result is consistent with the notion that the understory plays a crucial role in the structural and functional complexity of more open forest ecosystems (Aoki, 2012; Lin, 2015). For example, C_4 grasses and oak species at the xeric site were better adapted to drought (Osborne and Sack, 2012; Roman et al., 2015), which enabled high quality entropy production and the maintenance of its structural integrity (i.e., lower decreases in EVI; Fig. 1). We found further support for this trend in the steep increase in J_{NEE}, eff_M, and eff_s with greater EVI at the xeric site, suggesting that greater plant biomass and leaf area increased ecosystem function (Peng et al., 2017; Zhu et al., 2016) which allowed for higher quality entropy production. For instance, high overstory oak abundance at the xeric site (~20 %) in addition to the C_4 understory resulted in more transpiration during spring and summer, as well as during drought (i.e., anisohydric response; Roman et al., 2015), compared to stands containing just pine trees (Klein et al., 2013; Renninger et al., 2015; Stoy et al., 2006). This led to similar entropy efficiencies compared to the mesic site, as evidenced by both sites having comparable eff_s, even though B_A was substantially lower (Table 1).

Our results demonstrate the role of active biological functions in controlling energy and entropy fluxes in ecosystems, in addition to the underlying reflective capacities of the land surface (i.e., albedo; Stoy et al., 2014). For example, higher energy use efficiency during drought and low SWC (eff_M, Fig. 7) at the xeric site suggests an evolutionary adaptation of the plant species to low soil water availability and high VPD (Basu et al., 2016; Brodribb et al., 2014). In contrast, plant species at the mesic were adapted to higher soil water conditions, such that eff_s decreased, as the quality of entropy dissipation through other fluxes leads to lower J_{LE} (Kuricheva et al., 2017). This is because J_{LE} couples both mass and heat dynamics (Brunsell et al., 2011), whereas J_H is only a function of the thermal gradient (Kleidon, 2010; LeMone et al., 2007). Nevertheless, J_H increased at all sites during the first year of drought and then remained higher compared to pre-drought conditions, indicating a shift of ecological function (Ban-Weiss et al., 2011) towards lower quality energy degradation at all sites (Kuricheva et al., 2017). However, the rapid increase in J_{LE} and decrease in albedo in 2012 at the mesic and xeric sites indicated ecosystem recovery. This provides evidence of rapid adaptation of the plant canopy to drought, which allowed for greater eff_{rad}. Nevertheless, the xeric site was less efficient in using available radiation energy, indicated by high $R_{l,out}$ (Brunsell et al., 2011), as well as a higher albedo compared to the mesic site. Structural limitations due to lower productivity (i.e., lower EVI), a consequence of the sandy soil characteristics at the site, impeded the efficient absorption of available radiation, therefore lowering eff_{rad} (Norris et al., 2011). One reason for this lower entropy efficiency at the site was the large

proportion of deciduous oak trees (Table 1), which typically shed their leaves during the winter and therefore decrease the absorptive capacity (Baldocchi et al., 2004). However, high eff_s relative to the intermediate site indicated that the xeric site was using the remaining energy available to the site more efficiently. These results demonstrate that sites with higher biodiversity are better adapted to changes in resource availability by way of how they alter their reflective properties, such that energy partitioning is optimized (i.e., high absorption of solar radiation) and high entropy production can be maintained (Gunawardena et al., 2017; Otto et al., 2014; Taha et al., 1988).

We found support for our second hypothesis, that entropy efficiencies (cumulative sums of eff_{rad}, eff_M and eff_s) are higher at more biodiverse sites (i.e., mesic site). Accordingly, the mesic site efficiently used available energy from incoming solar radiation (Fig. 2) through lower reflection of R_s and by emitting less longwave radiation (Lin, 2015). This suggests higher ecological function of the plant species, especially longleaf pine in the overstory and wiregrass in the understory. Wiregrass is a C_4 species that can maintain photosynthetic rates under high temperatures (Osborne and Sack, 2012; Ward et al., 1999), which allows for greater energy conversion and high-quality entropy dissipation (Brunsell et al., 2011). We confirmed these results at the xeric and mesic sites as indicated by J_{NEE} below 0 kJ m^{-2} K^{-1} when T_{air} increased. In contrast, the metabolism at the intermediate site was a source for entropy production when T_{air} was above 20 °C demonstrating an inefficiency in maintaining optimal function when environmental pressure was imposed on the system. This also demonstrates unsustainable entropy dissipation, as more energy was used to sustain metabolic function than was available. In contrast, greater metabolic efficiency at the mesic and xeric sites allowed for more rapid increases in the structural complexity at the sites as indicated by a steep decrease in albedo (Brunsell et al., 2011; Holdaway et al., 2010). The lower ability to adapt to changes in resource availability at the intermediate site could induce its degradation, if environmental fluctuations become more frequent and severe or air temperatures continue to rise with climate change (Mori, 2011; Siteur et al., 2016). This could further exacerbate instabilities for nearby sites, as changes in the reflective properties of degraded sites can alter microclimate and weather patterns across whole ecosystems (Norris et al., 2011).

In contrast to the mesic and xeric sites, metabolic activity at the intermediate site was largely dependent on EVI (i.e., leaf area and biomass), demonstrating lower biological control of individual plant species (i.e., stomatal control; Urban et al. 2016), but a strong influence of the amount of biomass, and therefore higher photosynthetic capacity, present at the site (Brunsell et al., 2011; Fig. 4 and 6). For example, even though the increase in EVI in 2012 was greater at the intermediate site (Fig. 1) this did not correspond to higher J_{LE} or a decrease in albedo. To illustrate, the intermediate site was unable to maintain negative metabolic entropy production, when biomass was below a certain threshold (EVI <0.35). This resulted in lower ecological function and lower quality entropy production, as energy was dissipated more through J_H, rather than J_{LE} (Brunsell et al., 2011). This reduced entropy efficiencies (eff_{rad}, eff_M and eff_s) at the site when contrasted to the mesic and xeric sites (Fig. 6 and 7), which affected its recovery from drought. In contrast, the mesic site was able to maintain a negative value when EVI was ≥ 0.2, indicating greater adaptive capacity of individual plant species, which "rescued" ecosystem function (Elmqvist et al., 2003). Our third hypothesis was therefore partially supported, as the intermediate site had lower eff_M and eff_s. Although eff_{rad}, as an indicator for ecosystem radiation efficiency, showed that the intermediate site was more

efficient in using available energy and producing entropy compared to the xeric site; it did not acclimate eff_{rad} to changes in SWC (Fig. 7), which resulted in slower adaptation to drought. The result of lower eff_M and eff_s at the intermediate site is intriguing as the mesic and intermediate sites were structurally similar, based on similar B_A, mean DBH and overstory tree compositions (Table 1). The inefficiency was a consequence of anthropogenic modification, which homogenized the ecosystem, leading to a decrease in biodiversity (Table. 1; Fig. 3). This was a results of soil perturbations from anthropogenic management that took place prior to its establishment (>95 years ago). This suggests that lower plant biodiversity at the site decreased ecological function, which reduced entropy efficiency and therefore resilience to disturbance (Meysman and Bruers, 2010). This was especially apparent when plant biomass was low (low EVI = low J_{NEE} and lower overall J_{LE}), such that plant functional types present at the site could not rescue ecosystem function during disturbance (Elmqvist et al., 2003)1.

We conclude that the quality of entropy fluxes, in relation to structural and environmental variables gives valuable insights into the functional complexity of ecosystems and their ability to adapt to drought. Furthermore, a combination of different entropy efficiency ratios revealed how structural and/or functional characteristics affect energy efficiencies in ecosystems. Our results demonstrate that ecosystem resilience was mediated by ecosystem entropy efficiency, which was a function of plant biodiversity and ecosystem structure, as well as anthropogenic legacy. We show that low ecological function at anthropogenically altered sites has the potential to decrease ecosystem function, and therefore inhibit optimal energy use efficiency (Meysman and Bruers, 2010), especially with disturbances events. Changes in climate and natural and human induced disturbances are becoming more frequent and severe (IPCC, 2014), demanding more predictive power about how changes in ecosystem structure and function will alter resilience to disturbances. Future policy, conservation or restoration applications depend on reliable theories such as the theory of MEP presented here, to maintain ecosystem services and ecological function (Haddeland et al., 2014; Porter et al., 2012; Reinmann and Hutyra, 2016; Thom et al., 2017). This is especially critical for anthropogenically modified systems, as their land use history can affect changes in energy use efficiency and thus alter their ability to recover from disturbances (Bürgi et al., 2016; Foster et al., 2003). The application of MEP theory could improve our understanding of the interaction of structure, function and legacy on energy use efficiency across a variety of global ecosystems.

Author contribution

G.S. and L.B. designed and acquired funding for the research. S.W. and C.S. analyzed the data. P.S. aided S.W. with the theories of MEP and energy density. All authors contributed to writing of the manuscript.

Acknowledgement

The authors thank the Forest Ecology laboratories personnel, with special thanks to Tanner Warren, Andres Baron-Lopez and Scott Taylor, for data collection and provision during the study at the Joseph W. Jones Ecological Research Center. CS and GS acknowledge support from the U.S. National Science Foundation (DEB EF-1241881). PS acknowledges support from the U.S. National Science Foundation (DEB 1552976, and 1702029) and the USDA National Institute of Food and Agriculture (Hatch project 228396).

References

Abu-Hamdeh, N. H.: Thermal properties of soils as affected by density and water content, Biosystems Engineering, 86(1), 97–102, doi:10.1016/s1537-5110(03)00112-0, 2003.

Amthor, J. S.: From sunlight to phytomass: On the potential efficiency of converting solar radiation to phyto-energy, New Phyt., 188(4), 939–959, doi:10.1111/j.1469-8137.2010.03505.x, 2010.

Aoki, I.: Entropy Principle in Living Systems (Min–Max Principle), Entropy Principle for the Development of Complex Biotic Systems, (Chapter 2), 87–88, doi:10.1016/B978-0-12-391493-4.00008-1, 2012.

Baldocchi, D. D., Xu, L. and Kiang, N.: How plant functional-type, weather, seasonal drought, and soil physical properties alter water and energy fluxes of an oak–grass savanna and an annual grassland, Agric. For. Meteorol., 123(1-2), 13–39, doi:10.1016/j.agrformet.2003.11.006, 2004.

Ban-Weiss, G. A., Bala, G., Cao, L., Pongratz, J. and Caldeira, K.: Climate forcing and response to idealized changes in surface latent and sensible heat, Environ. Res. Lett., 6(3), 034032, doi:10.1088/1748-9326/6/3/034032, 2011.

Basu, S., Ramegowda, V., Kumar, A. and Pereira, A.: Plant adaptation to drought stress, F1000Research, 5(0), 1554, doi:10.12688/f1000research.7678.1, 2016.

Beer, C., Ciais, P., Reichstein, M., Baldocchi, D., Law, B. E., Papale, D., Soussana, J. F., Ammann, C., Buchmann, N., Frank, D., Gianelle, D., Janssens, I. A., Knohl, A., Köstner, B., Moors, E., Roupsard, O., Verbeeck, H., Vesala, T., Williams, C. A. and Wohlfahrt, G.: Temporal and among-site variability of inherent water use efficiency at the ecosystem level, Global Biogeochem. Cycles, 23(2), n/a–n/a, doi:10.1029/2008GB003233, 2009.

Bohn, F. J. and Huth, A.: The importance of forest structure to biodiversity–productivity relationships, R. Soc. open sci., 4(1), 160521, doi:10.1098/rsos.160521, 2017.

Brodribb, T. J., McAdam, S. A. M., Jordan, G. J. and Martins, S. C. V.: Conifer species adapt to low-rainfall climates by following one of two divergent pathways, Proc Natl Acad Sci USA, 111(40), 14489–14493, doi:10.1073/pnas.1407930111, 2014.

Brookes, J. D., Aldridge, K., Wallace, T., Linden, L. and Ganf, G. G.: Multiple interception pathways for resource utilisation and increased ecosystem resilience, Hydrobiologia, 552(1), 135–146, doi:10.1007/s10750-005-1511-8, 2005.

Brunsell, N. A., Schymanski, S. J. and Kleidon, A.: Quantifying the thermodynamic entropy budget of the land surface: Is this useful? Earth Sys. Dyn., 2(1), 87–103, 2011.

Bürgi, M., Östlund, L. and Mladenoff, D. J.: Legacy effects of human land use: Ecosystems as time-lagged systems, Ecosystems, 20(1), 94–103, doi:10.1007/s10021-016-0051-6, 2016.

Campbell, G. S. and Norman, C. G.: An introduction to environmental biophysics, Springer Science & Business Media. 1998.

Clement, R.: EdiRe data software, School of Geosciences, The University of Edinburgh, Edinburgh, Scotland. 1999.

Cochran, F. V., Brunsell, N. A. and Suyker, A. E.: A thermodynamic approach for assessing agroecosystem sustainability, Ecol. Indic., 67, 204–214, doi:10.1016/j.ecolind.2016.01.045, 2016.

DAAC, O.: MODIS collection 5 land products global subsetting and visualization tool: MOD13Q1 MODIS/Terra and MYD13Q1 MODIS/Aqua Vegetation Indices, NASA EOSDIS Land Processes DAAC, USGS Earth Resources Observation and Science EROS Center, 2008.

Dai, A., Qian, T., Dai, A., Trenberth, K. E. and Qian, T.: A Global Dataset of Palmer Drought Severity Index for 1870–2002: Relationship with Soil Moisture and Effects of Surface Warming, http://dx.doi.org/10.1175/JHM-386.1, 5(6), 1117–1130, doi:10.1175/JHM-386.1, 2004.

Dantas-Torres, F.: Climate change, biodiversity, ticks and tick-borne diseases: The butterfly effect, International Journal for Parasitology: Parasites and Wildlife, 4(3), 452–461, doi:10.1016/j.ijppaw.2015.07.001, 2015.

Dewar, R. C.: Maximum entropy production and the fluctuation theorem, J. Phys. A: Math. Gen., 38(21), L371–L381, doi:10.1088/0305-4470/38/21/L01, 2005.

Dyke, J. and Kleidon, A.: The maximum entropy production principle: Its theoretical foundations and applications to the Earth system, Entropy, 12(3), 613–630, doi:10.3390/e12030613, 2010.

Elmqvist, T., Folke, C., Nyström, M., Peterson, G., Bengtsson, J., Walker, B. and Norberg, J.: Response diversity, ecosystem change, and resilience, Front. Ecol. Environ., 1(9), 488–494, doi:10.1890/1540-9295(2003)001[0488:RDECAR]2.0.CO;2, 2003.

Endres, R. G.: Entropy production selects nonequilibrium states in multistable systems, Sci. Rep., 7(1), 1–13, doi:10.1038/s41598-017-14485-8, 2017.

England, J. L.: Dissipative adaptation in driven self-assembly, Nature nanotechnology, 10(11), 919–923, doi:10.1038/nnano.2015.250, 2015.

Finzi, A. C., Norby, R. J., Calfapietra, C., Gallet-Budynek, A., Gielen, B., Holmes, W. E., Hoosbeek, M. R., Iversen, C. M., Jackson, R. B., Kubiske, M. E., Ledford, J., Liberloo, M., Oren, R., Polle, A., Pritchard, S., Zak, D. R., Schlesinger, W. H. and Ceulemans, R.: Increases in nitrogen uptake rather than nitrogen-use efficiency support higher rates of temperate forest productivity under elevated CO_2, Proc Natl Acad Sci USA, 104(35), 14014–14019, doi:10.1073/pnas.0706518104, 2007.

Foster, D., Swanson, F., Aber, J., Burke, I., Brokaw, N., Tilman, D. and Knapp, A.: The importance of land-use legacies to ecology and conservation, BioScience, 53(1), 77–88, doi:10.1641/0006-3568(2003)053[0077:TIOLUL]2.0.CO;2, 2003.

Fox, J. and Weisberg, S.: car: Companion to Applied Regression, Second Edition. Thousand Oaks CA, 2011.

Franklin, J., Serra-Diaz, J. M., Syphard, A. D. and Regan, H. M.: Global change and terrestrial plant community dynamics, Proc Natl Acad Sci USA, 113(14), 3725–3734, doi:10.1073/pnas.1519911113, 2016.

Goebel, P. C., Palik, B. J., Kirkman, L. K. and West, L.: Field guide: landscape ecosystem types of Ichauway. Joseph W. Jones Ecological Research Center at Ichauway, Newton, Report number 97–1. 1997.

Goebel, P. C., Palik, B. J., Kirkman, L. K., Drew, M. B., West, L. and Pederson, D. C.: Forest ecosystems of a Lower Gulf Coastal Plain landscape: Multifactor classification and analysis, J. Torrey Bot. Soc., 128(1), 47, doi:10.2307/3088659, 2001.

Gunawardena, K. R., Wells, M. J. and Kershaw, T.: Utilising green and bluespace to mitigate urban heat island intensity, Science of the Total Environment, The, 584-585, 1040–1055, doi:10.1016/j.scitotenv.2017.01.158, 2017.

Haddeland, I., Heinke, J., Biemans, H., Eisner, S., Flörke, M., Hanasaki, N., Konzmann, M., Ludwig, F., Masaki, Y., Schewe, J., Stacke, T., Tessler, Z. D., Wada, Y. and Wisser, D.: Global water resources affected by human interventions and climate change, Proc Natl Acad Sci USA, 111(9), 3251–3256, doi:10.1073/pnas.1222475110, 2014.

Hardiman, B. S., Bohrer, G., Gough, C. M., Vogel, C. S. and Curtis, P. S.: The role of canopy structural complexity in wood net primary production of a maturing northern deciduous forest, Ecology, 92(9), 1818–1827, doi:10.1890/10-2192.1, 2011.

Hastings, A.: Chaos in Ecology: Is Mother Nature a Strange Attractor? Annual review of ecology and systematics, 24(1), 1–33, doi:10.1146/annurev.ecolsys.24.1.1, 1993.

Holdaway, R. J., Sparrow, A. D. and Coomes, D. A.: Trends in entropy production during ecosystem development in the Amazon Basin, Philos T Roy Soc B, 1437–1447, doi:10.1098/rstb.2009.0298, 2010.

Huryna, H. and Pokorny, J.: The role of water and vegetation in the distribution of solar energy and local climate: a review, Folia Geobotanica, 51(3), 191–208, doi:10.1007/s12224-016-9261-0, 2016.

IPCC: Climate Change 2014: Synthesis Report. Contribution of Working Groups I, II and III to the Fifth Assessment Report of the Intergovernmental Panel on Climate Change, edited by Core Writing Team, R. K. Pachauri, and L. A. Meyer, IPCC, Geneva. 2014.

Jaynes, E. T.: Information theory and statistical mechanics. II, Phys. Rev., 108(2), 171–190, doi:10.1103/PhysRev.108.171, 1957a.

Jaynes, E. T.: Information theory and statistical mechanics, Phys. Rev., 106(4), 620–630, doi:10.1103/PhysRev.106.620, 1957b.

Juang, J.-Y., Katul, G., Siqueira, M., Stoy, P. and Novick, K.: Separating the effects of albedo from eco-physiological changes on surface temperature along a successional chronosequence in the southeastern United States, Geophys Res Lett, 34, 1–5, doi:10.1029/2007GL031296, 2007.

Kaimal, J. C. and Gaynor, J. E.: Another look at sonic thermometry, Boundary-Layer Meteorol, 56(4), 401–410, doi:10.1007/BF00119215, 1991.

Kang, M., Zhang, Z., Noormets, A., Fang, X., Zha, T., Zhou, J., Sun, G., McNulty, S. G. and Chen, J.: Energy partitioning and surface resistance of a poplar plantation in northern China, Biogeosciences, 12(14), 4245–4259, doi:10.5194/bg-12-4245-2015, 2015.

Kim, Y. and Wang, G.: Soil moisture-vegetation-precipitation feedback over North America: Its sensitivity to soil moisture climatology, Journal of Geophysical Research Atmospheres, 117(17), 1–18, doi:10.1029/2012JD017584, 2012.

Kirkman, L. K., Giencke, L. M., Taylor, R. S., Boring, L. R., Staudhammer, C. L. and Mitchel, R. J.: Productivity and species richness in longleaf pine woodlands: Resource-disturbance influences across an edaphic gradient, Ecology, 97(9), 2259–2271, doi:10.1002/ecy.1456, 2016.

Kirkman, L. K., Mitchell, R. J., Helton, R. C. and Drew, M. B.: Productivity and species richness across an environmental gradient in a fire-dependent ecosystem, Am. J. Bot., 88(11), 2119–2128, 2001.

Kleidon, A.: A basic introduction to the thermodynamics of the Earth system far from equilibrium and maximum entropy production, Philos T Roy Soc B, 365(1545), 1303–1315, doi:10.1098/rstb.2009.0310, 2010.

Kleidon, A., Malhi, Y. and Cox, P. M.: Maximum entropy production in environmental and ecological systems, Philos T Roy Soc B, 365(1545), 1297–1302, doi:10.1098/rstb.2010.0018, 2010.

Klein, T., Shpringer, I., Ben Fikler, Elbaz, G., Cohen, S. and Yakir, D.: Relationships between stomatal regulation, water-use, and water-use efficiency of two coexisting key Mediterranean tree species, For. Ecol. Manage., 302, 34–42, doi:10.1016/j.foreco.2013.03.044, 2013.

Kuricheva, O., Mamkin, V., Sandlersky, R., Puzachenko, J., Varlagin, A. and Kurbatova, J.: Radiative entropy production along the paludification gradient in the southern taiga, Entropy, 19(1), 43, doi:10.3390/e19010043, 2017.

Lauri, P.-É., Marceron, A., Normand, F., Dambreville, A., Hortsys, U. P. R. and Island, R.: Soil water deficit decreases xylem conductance efficiency relative to leaf area and mass in the apple, The Journal of Plant Hydraulics, 1(Wery 2005), e0003, 2014.

LeMone, M. A., Chen, F., Alfieri, J. G., Tewari, M., Geerts, B., Miao, Q., Grossman, R. L. and Coulter, R. L.: Influence of land cover and soil moisture on the horizontal distribution of sensible and latent heat fluxes in southeast Kansas during IHOP_2002 and CASES-97, Journal of Hydrometeorology, 8(1), 68–87, doi:10.1175/JHM554.1, 2007.

Lenth, R. V.: Least-Squares Means: The R Package lsmeans, J. Stat. Soft., 69(1), doi:10.18637/jss.v069.i01, 2016.

Lin, H.: Thermodynamic entropy fluxes reflect ecosystem characteristics and succession, Ecol. Model., 298, 75–86, doi:10.1016/j.ecolmodel.2014.10.024, 2015.

Marín, D., Martín, M., Serrot, P. H. and Sabater, B.: Thermodynamic balance of photosynthesis and transpiration at increasing CO2 concentrations and rapid light fluctuations, BioSystems, 116, 21–26, doi:10.1016/j.biosystems.2013.12.003, 2014.

Meysman, F. J. R. and Bruers, S.: Ecosystem functioning and maximum entropy production: a quantitative test of hypotheses, Philos T Roy Soc B, 365(1545), 1405–1416, doi:10.1098/rstb.2009.0300, 2010.

Mori, A. S.: Ecosystem management based on natural disturbances: Hierarchical context and non-equilibrium paradigm, Journal of Applied Ecology, 48(2), 280–292, doi:10.1111/j.1365-2664.2010.01956.x, 2011.

Müller, F. and Kroll, F.: Integrating ecosystem theories - Gradients and orientors as outcomes of self-organized processes, International Journal of Design and Nature and Ecodynamics, 6(4), 318–341, doi:10.2495/DNE-V6-N4-318-341, 2011.

NCDC: Monthly Station Normals of Temperature, Precipitation, and Heating and Cooling Degree Days 1981–2010, National Climatic Data center, Asheville, NC. 2011.

Nikolov, N. T., Massman, W. J. and Schoettle, A. W.: Coupling biochemical and biophysical processes at the leaf level: an equilibrium photosynthesis model for leaves of C_3 plants, Ecol. Model., 80(2-3), 205–235, doi:10.1016/0304-3800(94)00072-P, 1995.

Norris, C., Hobson, P. and Ibisch, P. L.: Microclimate and vegetation function as indicators of forest thermodynamic efficiency, Journal of Applied Ecology, 49(3), 562–570, doi:10.1111/j.1365-2664.2011.02084.x, 2011.

Odum, H. T.: Self-Organization, transformity, and information, Monthley Weather Review, 242(4882), 1132–1139, doi:10.1126/science.242.4882.1132, 1988.

Osborne, C. P. and Sack, L.: Evolution of C_4 plants: A new hypothesis for an interaction of CO_2 and water relations mediated by plant hydraulics, Philos T Roy Soc B, 367(1588), 583–600, doi:10.1098/rstb.2011.0261, 2012.

Otto, J., Berveiller, D., Bréon, F. M., Delpierre, N., Geppert, G., Granier, A., Jans, W., Knohl, A., Kuusk, A., Longdoz, B., Moors, E., Mund, M., Pinty, B., Schelhaas, M. J. and Luyssaert, S.: Forest summer albedo is sensitive to species and thinning: How should we account for this in Earth system models? Biogeosciences, 11(8), 2411–2427, doi:10.5194/bg-11-2411-2014, 2014.

Patzek, T. W.: Thermodynamics of agricultural sustainability: The case of US maize agriculture, Critical Reviews in Plant Sciences, 27(4), 272–293, doi:10.1080/07352680802247971, 2008.

Peng, S., Schmid, B., Haase, J. and Niklaus, P. A.: Leaf area increases with species richness in young experimental stands of subtropical trees, Journal of Plant Ecology, 10(1), 128–135, doi:10.1093/jpe/rtw016, 2017.

Perry, G. L. W.: Landscapes, space and equilibrium: shifting viewpoints, Progress in Physical Geography, 26(3), 339–359, doi:10.1191/0309133302pp341ra, 2002.

Pinheiro, J., Bates, D., DebRoy, S. and Sarkar, D.: "nlme" Linear and Nonlinear Mixed Effects Models, 3rd ed., 2014.

Porter, E. M., Bowman, W. D., Clark, C. M., Compton, J. E., Pardo, L. H. and Soong, J. L.: Interactive effects of anthropogenic nitrogen enrichment and climate change on terrestrial and aquatic biodiversity, Biogeochemistry, 114(1-3), 93–120, doi:10.1007/s10533-012-9803-3, 2012.

Reinmann, A. B. and Hutyra, L. R.: Edge effects enhance carbon uptake and its vulnerability to climate change in temperate broadleaf forests, Proc Natl Acad Sci USA, 114(1), 201612369–112, doi:10.1073/pnas.1612369114, 2016.

Renninger, H. J., Carlo, N. J., Clark, K. L. and Schäfer, K. V. R.: Resource use and efficiency, and stomatal responses to environmental drivers of oak and pine species in an Atlantic Coastal Plain forest, Front. Plant Sci., 6(103), 317, doi:10.3389/fpls.2015.00297, 2015.

Ripl, W.: Management of water cycle and energy flow for ecosystem control: the energy-transport-reaction (ETR) model, Ecol. Model., 78(1-2), 61–76, doi:10.1016/0304-3800(94)00118-2, 1995.

Roman, D. T., Novick, K. A., Brzostek, E. R., Dragoni, D., Rahman, F. and Phillips, R. P.: The role of isohydric and anisohydric species in determining ecosystem-scale response to severe drought, Oecologia, 179(3), 641–654, doi:10.1007/s00442-015-3380-9, 2015.

Schneider, E. D. and Kay, J. J.: Complexity and thermodynamics. Towards a new ecology, Futures, 26(6), 626–647, doi:10.1016/0016-3287(94)90034-5, 1994.

Siteur, K., Eppinga, M. B., Doelman, A., Siero, E. and Rietkerk, M.: Ecosystems off track: rate-induced critical transitions in ecological models, Oikos, 125(12), 1689–1699, doi:10.1111/oik.03112, 2016.

Starr, G., Staudhammer, C. L., Wiesner, S., Kunwor, S., Loescher, H. W., Baron, A. F., Whelan, A., Mitchell, R. J. and Boring, L.: Carbon Dynamics of Pinus palustris Ecosystems Following Drought, Forests, 7(5), 98, doi:10.3390/f7050098, 2016.

Steinborn, W. and Svirezhev, Y.: Entropy as an indicator of sustainability in agro-ecosystems: North Germany case study, Ecol. Model., 133(3), 247–257, doi:10.1016/S0304-3800(00)00323-9, 2000.

Stoy, P. C., Katul, G. G., Siqueira, M. B. S., Juang, J.-Y., Novick, K. A., McCarthy, H. R., C. Oishi, A., Uebelherr, J. M., Kim, H.-S. and Oren, R.: Separating the effects of climate and vegetation on evapotranspiration along a successional chronosequence in the southeastern US, Glob. Chang. Biol., 12(11), 2115–2135, doi:10.1111/j.1365-2486.2006.01244.x, 2006.

Stoy, P. C., Lin, H., Novick, K. A., Siqueira, M. B. S. and Juang, J.-Y.: The role of vegetation on the ecosystem radiative entropy budget and trends along ecological succession, Entropy, 16(7), 3710–3731, doi:10.3390/e16073710, 2014.

Svirezhev, Y. M.: Thermodynamics and ecology, Ecol. Model., 132(1-2), 11–22, doi:10.1016/S0304-3800(00)00301-X, 2000.

Swenson, R. O. D.: Emergent attractors and the law of maximum entropy production: Foundations to a theory of general evolution, Systems Research and Behavioral Science, 6(3), 187–197, 1989.

Taha, H., Akbari, H., Rosenfeld, A. and Huang, J.: Residential cooling loads and the urban heat island—the effects of albedo, Building and Environment, 23(4), 271–283, doi:10.1016/0360-1323(88)90033-9, 1988.

Thom, D., Rammer, W. and Seidl, R.: The impact of future forest dynamics on climate: interactive effects of changing vegetation and disturbance regimes, Ecol. Monogr., 87(4), 665–684, doi:10.1002/ecm.1272, 2017.

Thomas, R. T., Prentice, I. C., Graven, H., Ciais, P., Fisher, J. B., Hayes, D. J., Huang, M., Huntzinger, D. N., Ito, A., Jain, A., Mao, J., Michalak, A. M., Peng, S., Poulter, B., Ricciuto, D. M., Shi, X., Schwalm, C., Tian, H. and Zeng, N.: Increased light-use efficiency in northern terrestrial ecosystems indicated by CO_2 and greening observations, Geophysical Research Letters, 43(21), 11,339–11,349, doi:10.1002/2016GL070710, 2016.

Twine, T. E., Kustas, W. P., Norman, J. M., Cook, D. R., Houser, P. R., Meyers, T. P., Prueger, J. H. and Wesley, M. L.: Correcting eddy covariance flux underestimates over grassland, Agric. For. Meteorol., 103, 279–300, doi:10.1016/S0168-1923(00)00123-4, 2000.

Virgo, N. and Harvey, I.: Entropy Production in Ecosystems, in Advances in Artificial Life, vol. 4648, pp. 123–132, Springer, Berlin, Heidelberg. 2007.

Ward, J. K., Tissue, D. T., Thomas, R. B., and Strain, B. R.: Comparative responses of model C_3 and C_4 plants to drought in low and elevated CO_2, Glob. Chang. Biol., 5(8), 857–867, doi:10.1046/j.1365-2486.1999.00270.x, 1999.

Whelan, A., Mitchell, R., Staudhammer, C. and Starr, G.: Cyclic occurrence of fire and its role in carbon dynamics along an edaphic moisture gradient in longleaf pine ecosystems, edited by B. Bond-Lamberty, PLoS ONE, 8(1), e54045, doi:10.1371/journal.pone.0054045, 2013.

Whitfield, J.: Complex systems: Order out of chaos, Nature, 436(7053), 905–907, doi:10.1038/436905a, 2005.

Whitfield, J.: Survival of the likeliest? PLoS Biology, 5(5), e142, doi:10.1371/journal.pbio.0050142, 2007.

Wilson, K.: Energy balance closure at FLUXNET sites, Agric. For. Meteorol., 113(1-4), 223–243, doi:10.1016/S0168-1923(02)00109-0, 2002.

Woodward, G., Perkins, D. M. and Brown, L. E.: Climate change and freshwater ecosystems: impacts across multiple levels of organization, Philos T Roy Soc B, 365(1549), 2093–2106, doi:10.1098/rstb.2010.0055, 2010.

Zhu, J., Jiang, L. and Zhang, Y.: Relationships between functional diversity and aboveground biomass production in the Northern Tibetan alpine grasslands, Sci. Rep., 6(March), 1–8, doi:10.1038/srep34105, 2016.

Biogeosciences Discuss., https://doi.org/10.5194/bg-2018-322
Manuscript under review for journal Biogeosciences
Discussion started: 8 August 2018

Table 1: Stand characteristics at the mesic, intermediate and xeric sites at the Joseph W. Jones Ecological Research Center, Newton, GA, USA.

Characteristic	**Mesic**	**Intermediate**	**Xeric**
Mean DBH (cm)	25.9	42.5	22.5
B_A *P. palustris* (m^2 ha^{-1})	17.7	14.6	8.9
B_A all tree spp. (m^2 ha^{-1})	19.0	15.7	11.0
Proportion of oak overstory trees (%)	6.8	7.0	19.1
Wiregrass in the understory (%)	28	5	24
Woody species in the understory (%)	12	15	10

Biogeosciences Discuss., https://doi.org/10.5194/bg-2018-322
Manuscript under review for journal Biogeosciences
Discussion started: 8 August 2018

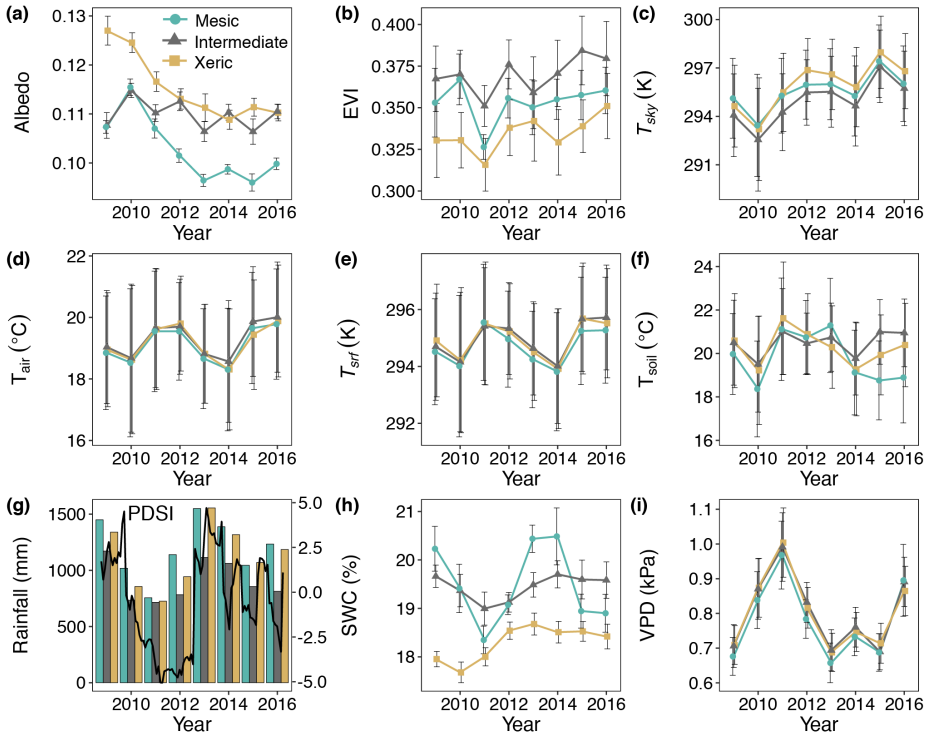

Figure 1: Environmental and structural variables for the years 2009-2016 at the mesic, intermediate and xeric sites, with monthly means of (a) albedo, (b) enhanced vegetation index (EVI), (c) surface temperature (T_{srf}), (d) air temperature (T_{air}), (e) sky temperature (T_{sky}), (f) soil temperature (T_{soil}), (g) average monthly rainfall sums and Palmer Drought Severity Index (PDSI), (h) soil moisture (SWC), as well as (i) vapor pressure deficit (VPD).

Biogeosciences Discuss., https://doi.org/10.5194/bg-2018-322
Manuscript under review for journal Biogeosciences
Discussion started: 8 August 2018

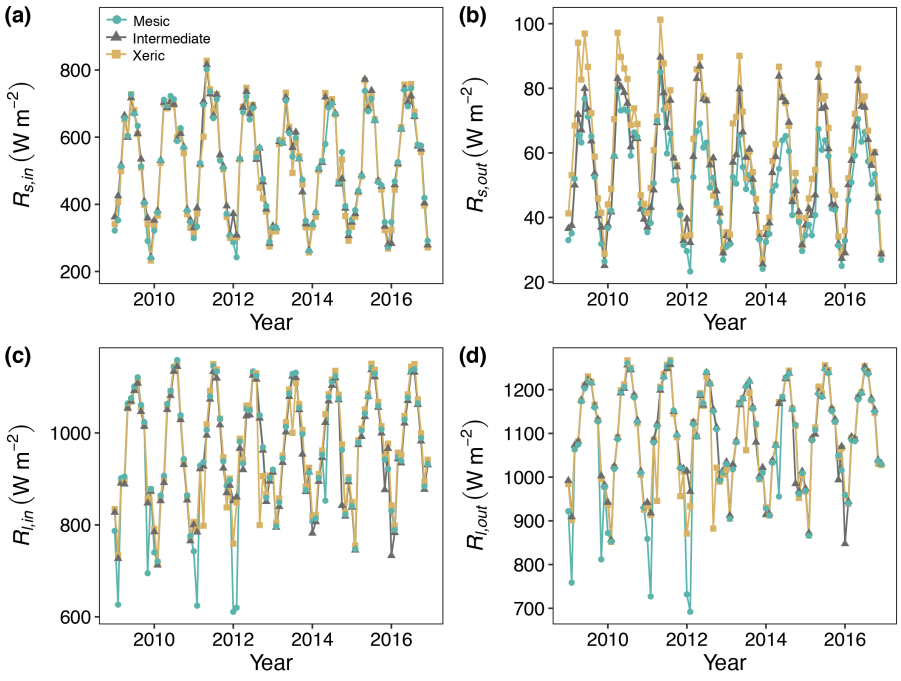

Figure 2: Incoming and outgoing longwave and shortwave radiation at the mesic, intermediate and xeric sites for the years 2009-2016, with monthly sums of (a) incoming shortwave radiation ($R_{s,in}$), (b) outgoing shortwave radiation ($R_{s,out}$), (c) incoming longwave radiation ($R_{l,in}$), and (d) outgoing shortwave radiation ($R_{l,out}$).

Figure 3: (a) Wiregrass and (b) woody understory biomass from 2009 through 2015 at the mesic, intermediate and xeric sites. Note that the sampling protocol changed to a 2-year measurements cycle in 2013, such that measurements were not made in 2014 and 2016.

Biogeosciences Discuss., https://doi.org/10.5194/bg-2018-322
Manuscript under review for journal Biogeosciences
Discussion started: 8 August 2018

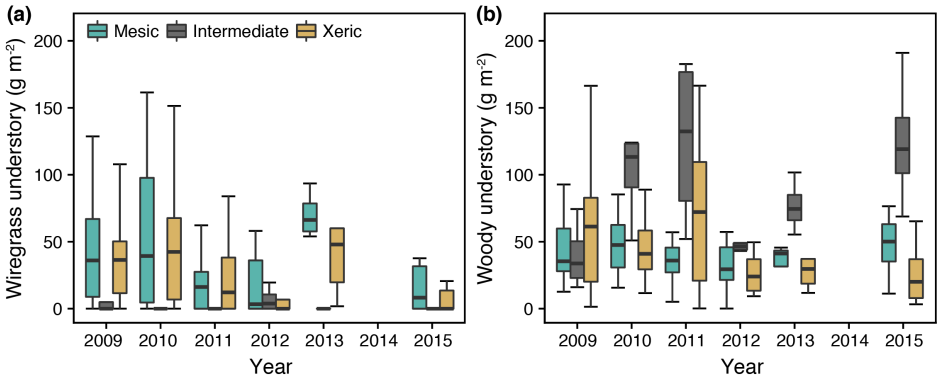

Figure 3: (a) Wiregrass and (b) woody understory biomass from 2009 through 2015 at the mesic, intermediate and xeric sites. Note that the sampling protocol changed to a 2-year measurements cycle in 2013, such that measurements were not made in 2014 and 2016.

Biogeosciences Discuss., https://doi.org/10.5194/bg-2018-322
Manuscript under review for journal Biogeosciences
Discussion started: 8 August 2018

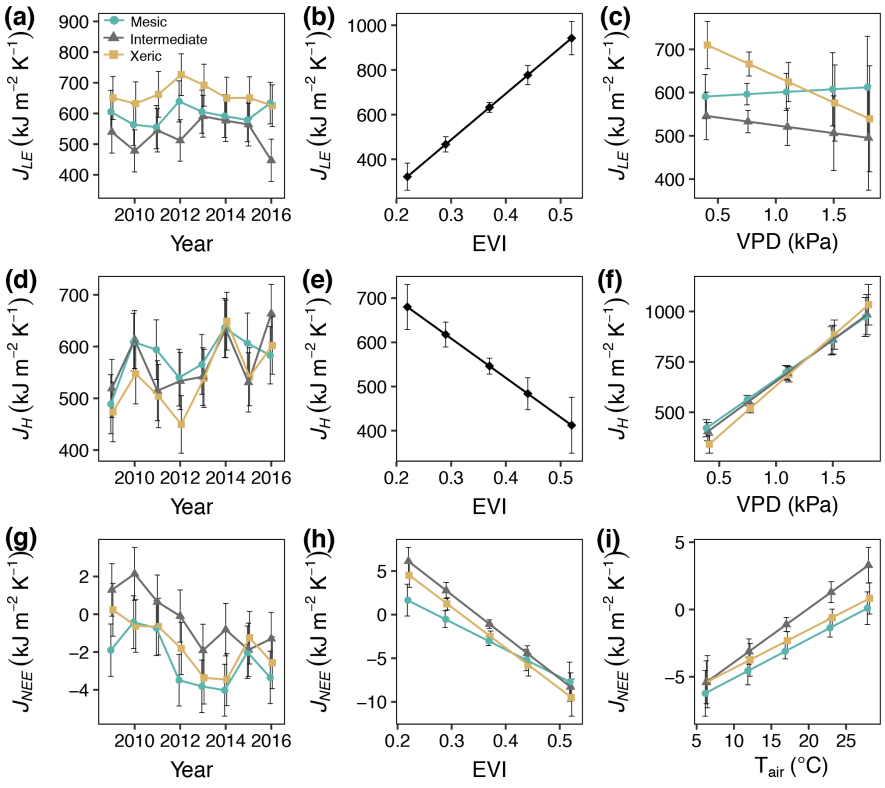

Figure 4: Annual changes of entropy fluxes of (a-c) latent energy (J_{LE}), (d-f) sensible heat (J_H), (g-i) metabolic entropy production (J_{NEE}), and their changes in interaction with site and (a, d, g) year, (b, e, h) Enhanced Vegetation Index (EVI) and (c, f) vapor pressure deficit (VPD) and (i) air temperature (T_{air}). For (b) and (e) the interaction with site was not significant.

Biogeosciences Discuss., https://doi.org/10.5194/bg-2018-322
Manuscript under review for journal Biogeosciences
Discussion started: 8 August 2018

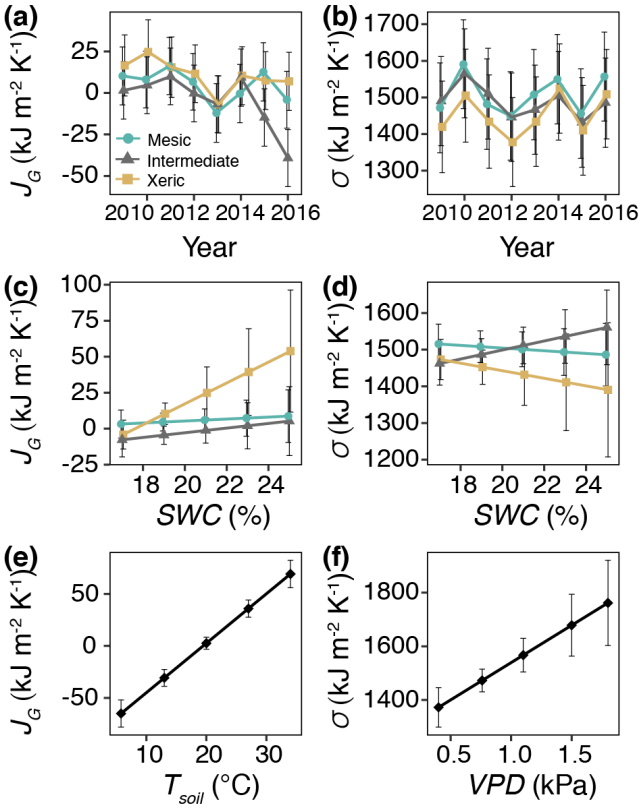

Figure 5: Annual changes of entropy fluxes of (a-c) ground heat flux (J_G), and (d-f) entropy production (σ), and their changes in interaction with site and (a and b) year, (c and d) soil water content (SWC) and (e) soil temperature (T_{soil}) and (f) vapor pressure deficit (VPD). For (e) and (f) the interaction with site was not significant.

Biogeosciences Discuss., https://doi.org/10.5194/bg-2018-322
Manuscript under review for journal Biogeosciences
Discussion started: 8 August 2018

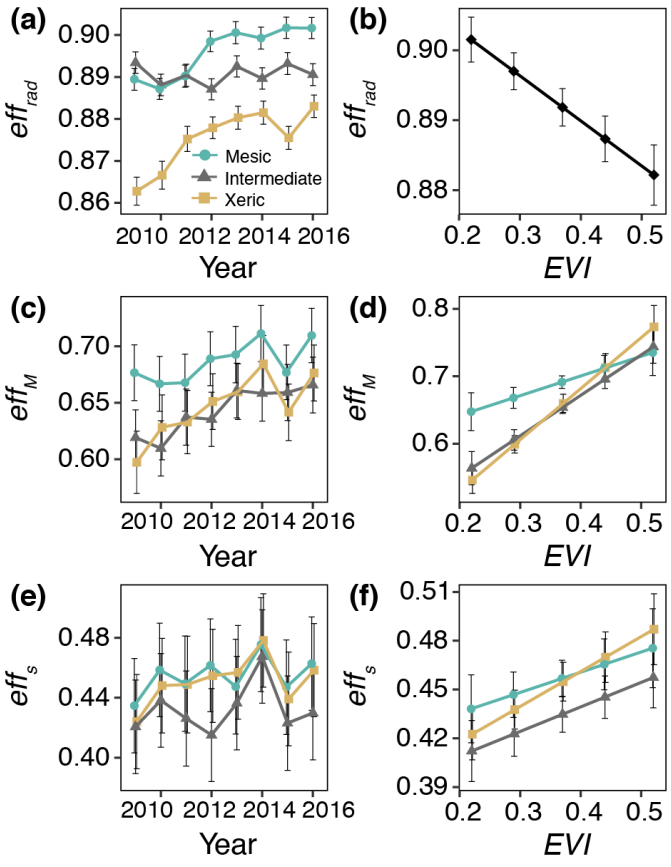

Figure 6: Mean monthly entropy efficiencies from 2009 through 2016 at the mesic, intermediate and xeric sites. (a and b) is the efficiency of the radiation budget (eff_{rad}), (c and d) the metabolic entropy efficiency (eff_M), and (e and f) the overall entropy efficiency (eff_s), as interactive effects of site and (a, c, e) year, (b, d, f) enhanced vegetation index (EVI). The interaction of site and EVI was not significant in (b).

Biogeosciences Discuss., https://doi.org/10.5194/bg-2018-322
Manuscript under review for journal Biogeosciences
Discussion started: 8 August 2018

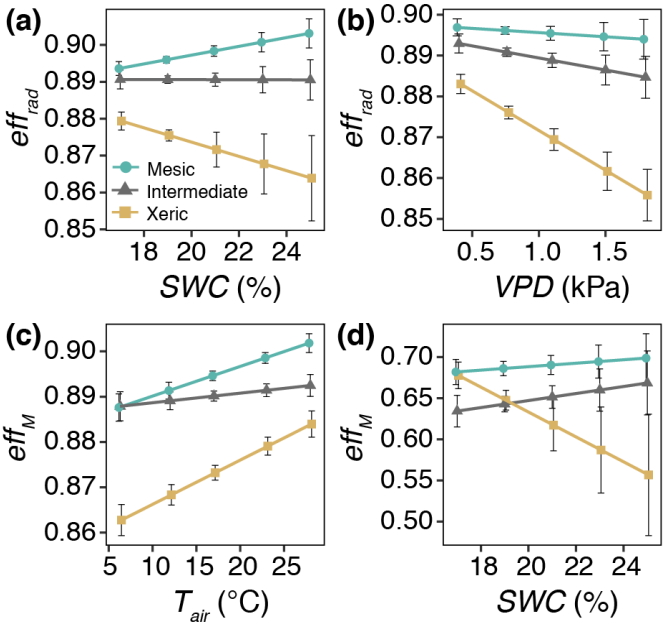

Figure 7: Differences in the entropy efficiencies by for radiation entropy efficiency (eff_{rad}) in interaction with site and (a) soil water content (SWC), (b) vapor pressure deficit (VPD), and (c) air temperature (T_{air}), as well as (d) metabolic entropy efficiency (eff_M) in interaction with site and SWC.